Colloid Polym Sci (2005) 283: 1163–1171
DOI 10.1007/s00396-005-1303-8

ORIGINAL CONTRIBUTION

Hiroyuki Kogure
Sunao Nanami
Yuka Masuda
Yoshiharu Toyama
Kenji Kubota

Hydration and dehydration behavior of *N*-isopropylacrylamide gel particles

Received: 23 October 2004
Accepted: 7 January 2005
Published online: 14 June 2005

H. Kogure · S. Nanami · Y. Masuda
Y. Toyama · K. Kubota (✉)
Department of Biological and Chemical Engineering Faculty
of Engineering,
Gunma University, Kiryu,
Gunma 376-8515, Japan
E-mail: kkubota@bce.gunma-u.ac.jp
Tel.: +81-277-301447

Abstract Thermal response of *N*-isopropylacrylamide (NiPAM) gel particles of submicron size was investigated by means of ultrasonic velocity and density focusing on the hydration and dehydration behavior. Hydration number, defined as the number of water molecules bound to one NiPAM monomer unit, was quantitatively evaluated in the course of the volume phase transition. Hydration numbers at low and high temperatures were about 7.5 (20 °C) and 3 (40 °C), respectively. Hydration number decreases markedly near the volume phase transition temperature, and the decrease is responsible to the formation of hydrophobic bonding and dehydration. The hydration number is independent both of the size and the composition of gel particles in the shrunken state, although there exists a composition dependence in the swollen state. It was also found that the self-assemblies formed by hydrophobic interaction are more bulky compared to those in the hydrated state.

Keywords NiPAM gel particles · Volume phase transition · Hydration number · Hydrophobic interaction · Ultrasonic velocity

Introduction

Volume phase transition is one of the most remarkable phenomena characteristic of the polymer gels [1–3]. The interplay of swelling pressure due to mixing entropy and deswelling pressure due to mixing interaction results in this kind of interesting phenomenon [4, 5]. *N*-isopropylacrylamide (NiPAM) gel is the most widely investigated among those gels, and an enormous number of investigations have been reported so far, especially relating to the development of functionalities [4–7]. The shrinking behavior of the elementary poly-NiPAM chains constructing the gel network, due to hydrophobic interaction, plays an essential role in this volume phase transition process, and the coil-to-globule transition of the elementary NiPAM polymer chains deeply correlates with the volume phase transition.

Coil-to-globule transition is the transition that takes place in a single chain [8–10]. If the interaction between adjacent chains is too strong compared to the intrachain interaction, it is difficult to observe a single chain transition because of predominant interchain aggregation. In organic solvents, van der Waals interaction is so weak that a macroscopic phase separation due to interchain transition precedes a single chain transition. On the contrary, in aqueous solutions, hydrophobic interaction and hydrogen bonding work additionally. It was previously found that an aqueous solution of linear poly-NiPAM (PNiPAM) exhibits a coil-to-globule transition

near its LCST type temperature [11–15]. Thereafter, many studies for PNiPAM relating to coil-to-globule transition have been reported so far [16–22]. According to analyses based on the Birshtein–Pryamitsyn theory [23, 24], two-body interaction in aqueous PNiPAM solution is much larger than in the case of organic solvents, for example poly(methylmethacrylate) in isoamyl acetate [19, 25, 26]. It is expected that hydrophobically self-assembled local domains interact effectively and result in sufficiently strong intrachain interaction. Hydrophobic interaction is the dominant factor in the volume phase transition of the hydrogels, as well as coil-to-globule transition in a single chain, and the characterization of hydrophobic interaction is quite important for the detailed analyses of those transitions. In fact, various studies on NiPAM hydrogels, for example fluorescence spectroscopic studies, have shown this fluorescence spectra, proving that hydrophobic circumstances correlate well with swelling-shrinking behavior, and it has been revealed that the dominant driving force of the volume phase transition is the hydrophobic interaction [27]. Maeda et al. [22] studied the hydration state during the coil-to-globule transition of aqueous PNiPAM solution using FT-IR spectroscopy, and found partial dehydration of the polymer chain and formation of intra- and interchain hydrogen bonding. They also argued that substantial hydrogen bonding remains even in the globule (shrunken) state, and the structure of water is determinant of the transition.

Several studies on the hydration of NiPAM hydrogel have been reported [20, 28–30]. Suetoh and Shibayama studied the non-uniform hydration in the thermal response of NiPAM gel by using DSC measurements, and found the unique dependence of thermal properties of NiPAM gel on the history of gel treatment [28]. Lele et al. [29] studied the bound water content in NiPAM gel theoretically and found that the bound water content at the shrunken state (high temperature) is about 0.4 g/g (hydration number $\sim$ 2.5), and increases three to four times at the swollen state. However, detailed and quantitative experiments focusing on the hydration behavior of NiPAM gel have not yet been reported.

Since the formation of hydrophobic bonding results in dehydration and the increase in free water molecules, quantitative evaluation of hydration/dehydration is needed for the analysis of the thermal response of NiPAM gel. However, such an analysis is difficult in practice for the macroscopic gels, because of the change in sample shape, heterogeneous internal structure, and spatial inhomogeneity brought in the thermal response [31, 32]. Instability due to such spatial inhomogeneity makes the thermal response of gels complicated. Since the spatial size of inhomogeneity should be in the order of submicrons [33–35], gel particles less than the spatial size of inhomogeneity are useful for such investigations, and the effect of inhomogeneity can be lessened. Moreover, the time to attain equilibrium is proportional to the square of the size of the gel, and it is convenient to use smaller size gel samples [36]. In addition, submicron size NiPAM gel particles are stable without the formation of any aggregation even at high temperature (shrinking region) [37]. Thus, we can examine the hydration-dehydration behavior of NiPAM gel in a stable equilibrium state.

Water molecules bound to solute particles are less compressible than free water molecules, and their content can be detected by ultrasonic velocity and density measurements, because the adiabatic compressibility is related to them. About 50 years ago, Shiio et al. [38] studied the binding of water to sugars and polymers using ultrasonic velocimetry. They assumed that bound water behaves similarly to ice in compression terms because they are hydrogen bonded, and it was found that bound water is almost dehydrated by the addition of alcohol (ethanol). Therefore, the compressibility of the polymer chain itself can be estimated according to their procedure, and it is possible to evaluate the bound water content or hydration number quantitatively by ultrasonic velocity combined with density measurements [38–42]. Similar dehydration behavior of NiPAM gel due to the addition of alcohol has been reported [43, 44].

In this paper, the hydration and dehydration behavior of NiPAM gel particles were characterized below and above the volume phase transition temperature. Three gel samples were prepared by the emulsion polymerization method: standard one, small sized ones, and ones with a higher content of *N,N′*-methylene bisacrylamide. Variation in particle size was monitored by dynamic light scattering (DLS). The procedure of evaluation of the hydration number from the ultrasonic velocity and density measurements is also described.

Materials and methods

Sample preparation

Gel Particles were prepared by the emulsion polymerization method above the volume phase transition temperature [37]. NiPAM monomer was purchased from Wako Chemicals, Japan, and was purified by successive recrystalization using hexane. *N,N′*-methylene bisacrylamide (BIS) was recrystalized from methanol. Ammonium persulfate (AP) as an initiator and sodium dodecylbenzenesulfonate (SD) as a dispersant were used without further purification. Pregel solution composed of 1.875 g NiPAM and 20 mg BIS dissolved in 30 g water was fully degassed, and dissolved oxygen was substituted by sufficient nitrogen. A necessary

Table 1 Composition at the preparation and hydrodynamic diameter at 20 °C

Code	NiPAM (g)	BIS (mg)	AP (mg)	SD (mg)	Water (g)	Diameter (nm)
NI-A	1.88	20	7.5	0.2	30	700
NI-B	1.88	20	7.5	20	30	200
NI-C	1.88	68	15	0.2	30	700

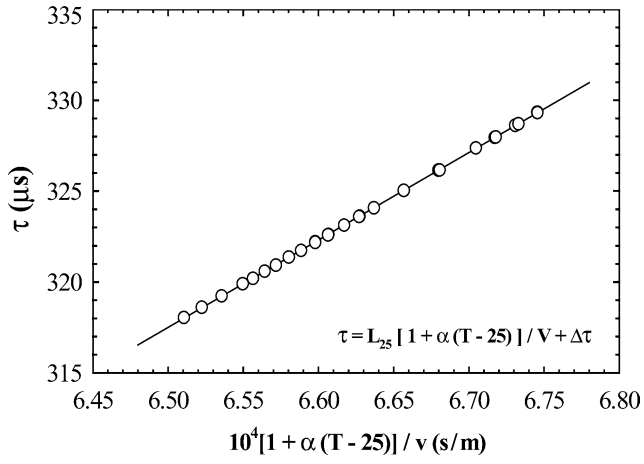

Fig. 1 Relationship of the period of sing-around signals with the reciprocal of sound velocity corrected for the thermal expansion of sample path length. Sample is water. The coefficient of determination is 0.99997

amount of SD was added (Table 1). The pregel solution was put into a vial equipped with a nitrogen bubbling tube and a magnetic stirrer and heated to 60 °C. The reaction was started by the addition of AP, and continued for 3 h with agitation under nitrogen. The reaction was terminated by the addition of methanol into the reaction vial. Then, the suspension was dialyzed thoroughly for 1 week against methanol and distilled water to remove the residual monomers and surfactant SD. Suspensions thus prepared were diluted to an appropriate concentration for measurement. Compositions and hydrodynamic diameters at 20 °C of the samples (code: NI-A, NI-B, and NI-C) prepared for the present study are shown in Table 1. Molar ratio of [NiPAM]/[BIS] is about 140 for NI-A. NI-B has a smaller size as a result of more SD in the preparation, and NI-C has a larger BIS content than NI-A.

Light scattering

Dynamic light scattering measurements were carried out using a homemade spectrometer and an ALV-5000 multiple-tau digital correlator to obtain the correlation function of the scattered light intensity $g^{(2)}(t)$ ($= \langle I(0) I(t) \rangle / \langle I(t) \rangle^2$ with $I(t)$ being the scattered light intensity at time t) and the hydrodynamic diameter as a function of temperature [45, 46]. Vertically polarized Ar ion laser operated at wavelength 488.0 nm was used as an incident beam. Correlation function $g^{(2)}(t)$ was analyzed by the use of the CONTIN method to obtain the decay time distribution function as follows:

$$g^{(2)}(t) - 1 = \left[\int A(\tau) \exp(-t/\tau) \mathrm{d}(\log \tau) \right]^2 \quad (1)$$

Here, τ is the decay time and $A(\tau)$ is the distribution function of the decay time. When only the translationally diffusional motion contributes to the correlation function, the hydrodynamic diameter D is simply obtained by the Stokes–Einstein equation, $D = (k_B T / 3\pi\eta) q^2$ τ. k_B, T, η, and q are the Boltzman constant, absolute temperature, solvent viscosity, and scattering vector defined as $q = (4\pi/\lambda)\sin(\theta/2)$ with λ and θ being the wavelength of the incident beam in the medium and the scattering angle, respectively. The z-averaged hydrodynamic diameter was obtained by use of $A(\tau)$. The concentration of gel particles was about 10 μg/cm^3, and the temperature was controlled within 5 mK.

Ultrasonic velocity

Ultrasonic velocity was measured by a sequential pulse oscillation method developed from the sing-around method [47, 48]. The resonant frequency of the transducer was 3 MHz. The time interval between the input and output signal was determined by a universal counter with the time resolution of 0.1 ns. Measurements were carried out at sample concentrations of about 5 mg/cm^3, and the cell length was about 5 cm. The measured period is related to the ultrasonic velocity by:

$$\tau = L_{25} \frac{1 + \alpha(T - 25)}{v} + \Delta\tau. \quad (2)$$

Here, τ, L_{25}, α, T, v, and $\Delta\tau$ are the period of the detected pulse sequence, cell length at 25 °C, thermal expansion coefficient of the cell, temperature, ultrasonic velocity, and the delay time due to the detecting circuit, respectively. Temperature constancy in the course of measurements was ±1 mK, and the reproducibility of velocity measurements was within 5×10^{-3} m/s.

The calibration curve of the homemade ultrasonic velocity measurement system is shown in Fig. 1. The reported values of ultrasonic velocity in pure water were used for the calibration [49]. The sing-around method should give a linear dependence of the period of the detected pulse signals upon the reciprocal of velocity with the correction of thermal expansion of path length. As shown in Fig. 1, very good linearity was obtained, and the delay time due to the electric circuit was evaluated from the fitting. The calibration constants thus determined were used to obtain the ultrasonic velocity.

Ultrasonic velocity in water in the experimental temperature region is about 1,500 m/s. Since the resonant frequency is 3 MHz, the wavelength is about 0.5 mm, being much larger (about 1,000 times) than the size of gel particles. Therefore, from the viewpoint of sound propagation, the sample solutions of gel particles can be regarded as continuous media, and the ultrasonic velocity affected only by the state of water.

In order to represent the variation of ultrasonic velocity in the solution compared to the solvent (water), the limiting velocity number defined as,

$$[v] = \lim \frac{(v/v_0 - 1)}{C} \quad (C \to 0) \tag{3}$$

was used. Here, v, v_0, and C are the ultrasonic velocity in the solution, that in the solvent, and the concentration of the sample, respectively. As the concentration used in the present study is sufficiently low, the difference between the experimentally determined values of $(v/v_0-1)/C$ and $[v]$ is negligibly small, and both can be treated equivalently.

Density

Density of the sample solutions was measured by the vibrating densitometer (DMA602, Anton Paar). Temperature constancy was ± 5 mK, and the reproducibility of density measurements was within 0.1 mg/cm^3. Measurements were performed at concentrations of less than 10 mg/cm^3.

In order to represent the variation of the solution density compared to the solvent, the limiting density number defined as

$$[\rho] = \lim \frac{(\rho/\rho_0 - 1)}{C} \quad (C \to 0) \tag{4}$$

was used. Here, ρ and ρ_0 are the density of the solution and of the solvent, respectively. Similarly to the case of ultrasonic velocity, no concentration dependence of $(\rho/\rho_0 - 1)/C$ was observed in the present experimental concentration.

Adiabatic compressibility β was calculated from the ultrasonic velocity v and the density ρ by the relation $\beta = 1/\rho V^2$.

Evaluation of hydration number

We consider that M_s g of solute particles is dissolved in V cm^3 of solution, according to the formulation of Shiio [38]. Concentration of the solution is given by $C = M_s/V$. Assuming that the additivity of volume, the total volume of solution V_t is the sum of free (unbound) water V_0, hydrated water V_h (which includes not only the hydrophobic hydration, but also the hydrophilic hydration, and the water molecules bound to the solute particles firmly), and solute V_s.

$$V_t = V_0 + V_h + V_s. \tag{5}$$

Usually it is considered that the states of water are classified into three: free water, hydrated (bound) water, and intermediate. A clear characterization of the intermediate state is, however, difficult and methods like the present ultrasonic measurement cannot detect the intermediate one by direct means. It should be noted that the present classification of water into two states (free and hydrated water) is still an approximate one. In addition, water molecules that surround solute particles but move almost freely, are not included in the hydrated water.

We define the density of free water ρ_0, hydrated water ρ_h, solute ρ_s, and the adiabatic compressibility of the solution β, free water β_0, hydrated water β_h, and solute β_s, respectively. Free water is considered the same as water itself. Then, $\beta = (-1/V_t)\,(\partial V_t/\partial P)_S$ is calculated as,

$$\frac{\beta}{\beta_0} = 1 + \frac{V_h}{M_s}\left(\frac{\beta_h}{\beta_0} - 1\right) + \frac{V_s}{M_s}\left(\frac{\beta_s}{\beta_0} - 1\right). \tag{6}$$

Using the representation of the limiting compressibility number defined as $[\beta] = (\beta/\beta_0 - 1)/C$, Eq. 6 is rewritten as

$$[\beta] = \frac{V_h}{M_s}\left(\frac{\beta_h}{\beta_0} - 1\right) + \frac{V_s}{M_s}\left(\frac{\beta_s}{\beta_0} - 1\right). \tag{7}$$

Principally, $[\beta]$ is defined as the limiting value to $C \to 0$. However, in dilute solutions like in the present case, no concentration dependence is observed, and the experimentally determined value of $(\beta/\beta_0 - 1)/C$ can be approximated to $[\beta]$ well enough, similar to the cases of $[v]$ and $[\rho]$. It should be noted that $[\beta]$ is equal to $-(2\,[v] + [\rho])$.

Hydration number S is defined as the number of water molecules bound to one NiPAM monomer unit, and then $S = \rho_h\,(m_s/m_w)\,(V_h/M_s)$ is written with m_w and m_s being the molecular weight of water and NiPAM monomer unit, respectively,

$$S = -\rho_h\left(\frac{m_s}{m_w}\right)\frac{[\beta] + (1/\rho_s)(1 - \beta_s/\beta_0)}{(1 - \beta_h/\beta_0)}. \tag{8}$$

By introducing the partial volume of solute V_s' defined as

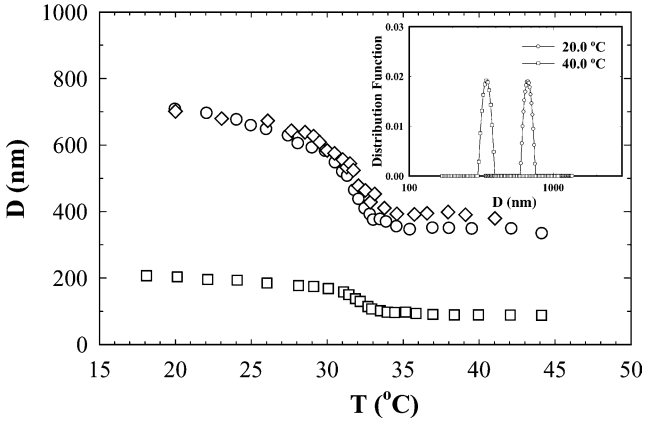

Fig. 2 Hydrodynamic diameter of NiPAM gel particle as a function of temperature. The symbols of *circle, square*, and *diamond* denote the sample NI-A, NI-B, and NI-C, respectively. The *inset* shows the distribution functions of the hydrodynamic diameter of the sample NI-A at the temperature 20.0 °C and 40.0 °C. Scattering angle was 30°

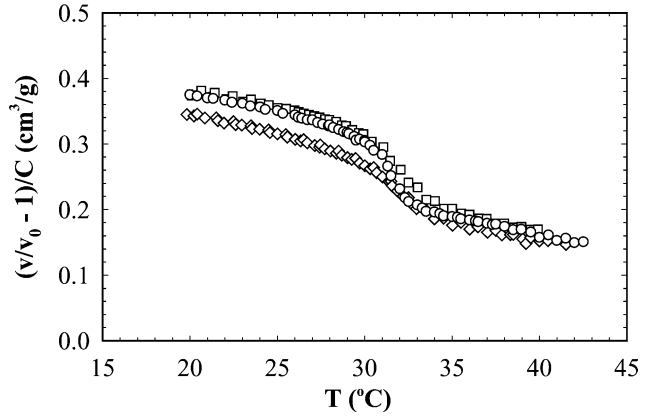

Fig. 3 Relationships of $(v/v_0 - 1)/C$ as a function of temperature. The meanings of the *symbols* are the same as those in Fig. 2

$$V_s' = \frac{1}{\rho_0} - [\rho] = \frac{1}{\rho_s} + \left(\frac{m_w}{m_s}\right) S \left(\frac{1}{\rho_h} - \frac{1}{\rho_0}\right) \tag{9}$$

Therefore, the hydration number S is formulated as,

$$S = -\rho_h \left(\frac{m_s}{m_w}\right) \left\{ \frac{[\beta] + V_s'(1 - \beta_s/\beta_0)}{[(1 - \beta_h/\beta_0) - (1 - \rho_h/\rho_0)(1 - \beta_s/\beta_0)]} \right\}. \tag{10}$$

It is noteworthy that the hydrated water content represented as the water mass per solute mass is given by (m_w/m_s) S.

The structure of hydrated (bound) water could be represented as that of ice without much error because hydration might be caused by hydrogen bonding principally, and ρ_h and β_h can be approximated by those of ice. The remaining unknown variable is β_s; if S becomes 0 during some conditions (all the hydrated water is excluded), β_s can be estimated from Eq. 10. Then, the hydration number S is obtainable from the experimentally observed quantities.

Results and discussion

Figure 2 depicts the swelling curves of three samples: NI-A, NI-B, and NI-C. The inset shows the distribution function of the hydrodynamic diameter of NI-A at the temperatures 20 °C and 40 °C. Hydrodynamic diameters were obtained by the Stokes-Einstein equation. It was ascertained that the present preparation of NiPAM gel particles gives very sharp size distribution. Almost the same shape of the distribution at high temperature as that at low temperature suggests that no aggregation had occurred. The sample solution was so dilute that no concentration dependence of the diameter determined by DLS measurements was detected. Radii of gyration were obtained simultaneously from the angular dependence of the scattered light intensity. The ratio of the radius of gyration to hydrodynamic radius is a little less than 0.78 (expected value for spheres of uniform density). Such a tendency may be related to the relatively large [NiPAM]/[BIS] ratio in the present preparation, and suggests that the present NiPAM gel particles are little core/shell type ones: that is, the outer shell part has a lower chain density and those chains expand loosely, while the inner core has a higher chain density.

At low temperature (say, < 30 °C), the diameter decreased monotonically with increase in temperature. Marked decrease in diameter occurred around 32 °C. This behavior corresponds to the volume phase transition observed in the macroscopic NiPAM gels. On the contrary, at high temperature (> 35 °C) almost no temperature dependence of the diameter was observed. Contrary to the case of the macroscopic NiPAM gels, the swelling curve was continuous. Continuous swelling behavior has been observed in NiPAM gel particles prepared at higher temperature than the phase separation temperature, similar to the present samples [14, 19, 50–53]. Although the diameters at 20 °C are almost the same for NI-A and NI-C, the diameters at the shrunken state are slightly different. NI-A with lower BIS content shrinks more than NI-C with higher BIS content. This is because the principal NiPAM chain constructing the gel network is longer in the case of the lower BIS content, and is likely to shrink further [13]. The sample NI-B has a much smaller diameter due to the larger amount of SD used in the preparation of the gel particle.

Figure 3 illustrates the relationships of $(v/v_0 - 1)/C$ as a function of temperature. Similar to the swelling curve in Fig. 2, continuous curves were obtained for all the samples. Marked decrease in $(v/v_0 - 1)/C$ was clearly observed near the volume phase transition temperature

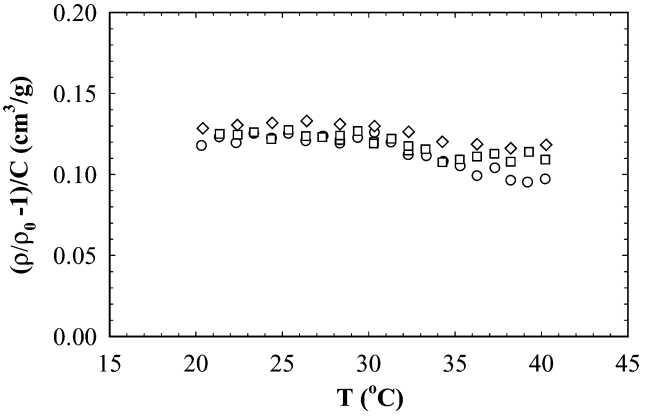

Fig. 4 Relationships of $(\rho/\rho_0 - 1)/C$ as a function of temperature. The meanings of the *symbols* are the same as those in Fig. 2

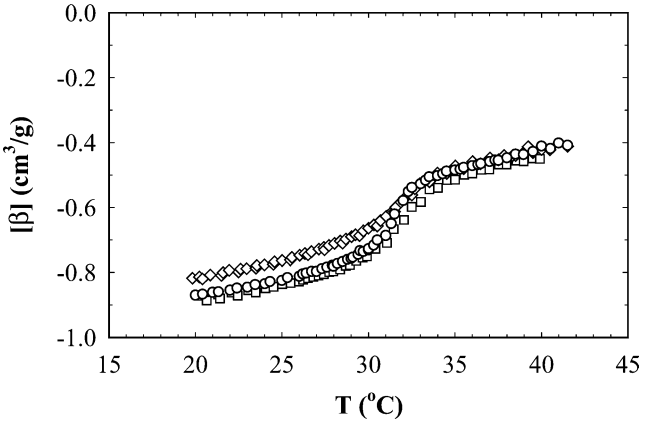

Fig. 5 Limiting compressibility number $[\beta]$ as a function of temperature. The meanings of the *symbols* are the same as those in Fig. 2

(ca. 32 °C). Although the magnitudes of $(v/v_0 - 1)/C$ vary with the preparations in the swollen state, they begin to coincide with each other in the shrunken state. Especially when the composition of NiPAM and BIS is the same (NI-A and NI-B), both curves are almost indistinguishable.

Figure 4 shows the temperature dependence of $(\rho/\rho_0 - 1)/C$. Continuous temperature dependence is again obtained, and a weak decrease at about 32 °C is observed in all the samples. It is worthy to note that the magnitudes of $(\rho/\rho_0 - 1)/C$ in the shrunken state are less than those in the swollen state. This means that the partial volume of the NiPAM chain in the shrunken state is larger than that of the swollen state according to Eq. 9, even though the elementary NiPAM chain composing the gel network shrinks. Since shrinkage results from the formation of hydrophobic self-assembling NiPAM monomer units and dehydration, the dehydrated assembly should be more bulky and have less density than that the hydrated state. This corresponds to the increase of partial molar volume of surfactant during the formation of micellar assembly by hydrophobic interaction [54, 55]. Moreover, pressure dependence of the coil-to-globule transition temperature for linear NiPAM polymer solution has been studied, and it has been reported that the transition temperature increases with pressure near the atmospheric pressure [56, 57]. The positive pressure dependence suggests the increase of partial volume of NiPAM monomer units in the course of transition, and is in good agreement with the present results. On the other hand, no definite increasing tendency of $(\rho/\rho_0 - 1)/C$ was observed in the temperature region above the volume phase transition temperature. This suggests that those dehydrated assemblies formed by hydrophobic interaction neither become more condensed with further increase in temperature, nor do they interact with the recombination of those assemblies.

Adiabatic compressibility β is related to the ultrasonic velocity v and the density $\rho$by the equation $\beta = 1/\rho V^2$. Resultant $[\beta]$ calculated from $(v/v_0 - 1)/C$ and $(\rho/\rho_0 - 1)/C$ are shown in Fig. 5. Here, the magnitudes of $(\rho/\rho_0 - 1)/C$ were interpolated from the experimental results in Fig. 4, because $(\rho/\rho_0 - 1)/C$ is less than those of $(v/v_0 - 1)/C$ and affects $[\beta]$ less. $[\beta]$ is negative in the experimental temperature range, and increases with temperature. Marked increase in $[\beta]$ occurs near the transition temperature. Although a variation in $[\beta]$ due to [NiPAM]/[BIS] composition is observed at low temperature, all the curves become superposed in the shrunken state.

In order to evaluate the hydration number using Eq. 10, it is necessary to determine β_s. Equation 10 can be rewritten as

$$[\beta] + \frac{1}{\rho_0} - [\rho] = \frac{\beta_s}{\beta_0}\left(\frac{1}{\rho_0} - [\rho]\right) - S\left(\frac{m_w}{m_s \rho_h}\right) \left[\left(1 - \frac{\beta_s}{\beta_0}\right) - \left(1 - \frac{\rho_h}{\rho_0}\right)\left(1 - \frac{\beta_s}{\beta_0}\right)\right]. \quad (11)$$

Therefore, if S can be ignored in some conditions β_s can be estimated. According to Shiio et al. [38], on the hydration behavior of saccharides and polyvinylalcohols in the mixed solvent of ethanol and water, it was found that the bound water is almost excluded at some ethanol compositions. In accordance with those facts, it has been found that NiPAM gel collapses to a minimum size in the mixed solvent of ethanol and water (co-non-solvency effect) [43, 44]. In that minimum state, all water should be dehydrated and the NiPAM chain shrunken.

Figure 6 shows the results of NI-A in the mixed solvent of ethanol and water at 25 °C. $[\beta]$ in panel (a) exhibits a maximum at the ethanol composition of ca. 30 v/v%. $[\beta] - [\rho] + 1/\rho_0$, and also shows a maximum behavior as shown in panel (b). The ethanol concentration for the maximum is in good agreement with the

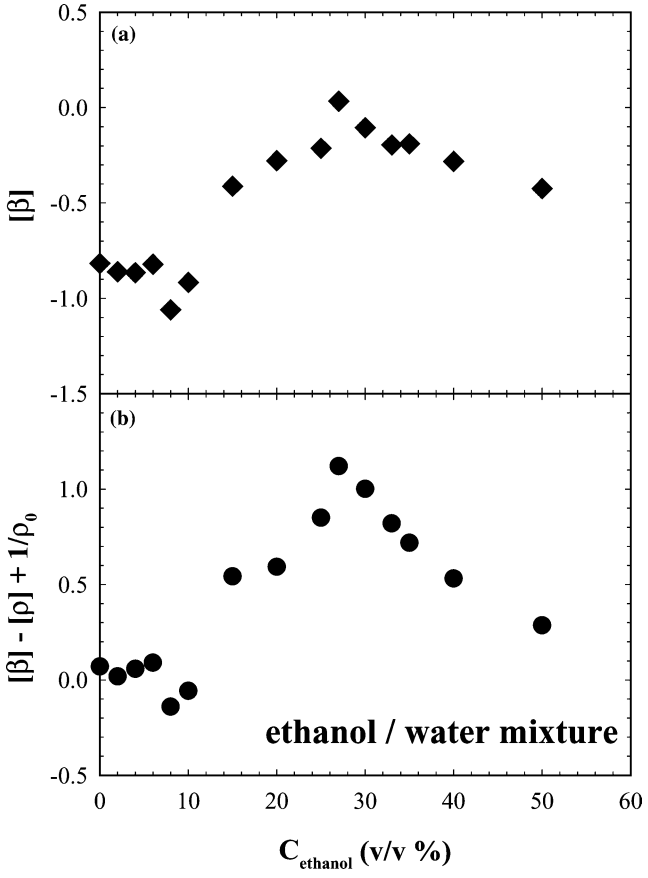

Fig. 6 [β] (*panel a*) and [β] − [ρ] + $1/\rho_0$ (*panel b*) of NiPAM gel particle suspension in the ethanol/water mixture as a function of the ethanol concentration (v/v%) at 25.0 °C

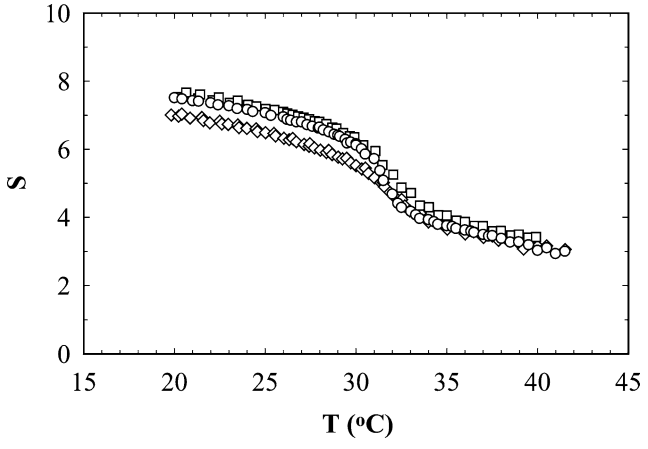

Fig. 7 Temperature dependence of the hydration number S. The meanings of the *symbols* are the same as those in Fig. 2

results of Zhu et al. [43] and Saunders et al. [44]. A decrease in the magnitude of [β] − [ρ] + $1/\rho_0$ with the ethanol composition above the concentration of maximum should be attributed to the solvation of ethanol to NiPAM chain. Thus, β_s of NiPAM chain was evaluated as 4 ($\pm$0.4)×10^{-10} Pa^{-1} using Eq. 11. This magnitude is comparable with that of water (4.5×10^{-10} Pa^{-1}), and is fairly larger than the reported value of 0.78×10^{-10} Pa^{-1} for the dry gel of NAPA/PAA (copolymer gel of sodium polyacrylate and polyacrylic acid, molar ratio = 3/1) by Koda et al. [40]. In our case, the NiPAM chain is in the liquid state and the larger value is reasonable. It should be noted that unrealistic negative values are obtained for the hydration number if the NiPAM chain is assumed to be incompressible (β_s = 0).

By using the value of β_s thus determined and assuming the values of ice for ρ_h and β_h, the hydration number S was evaluated as a function of temperature and is depicted in Fig. 7. Temperature dependence of β_s was ignored in the calculation. The experimental uncertainty of S is about 0.8. Hydration number decreases with the increase in temperature, and marked decrease is observed near the volume phase transition temperature of NiPAM gel (~32 °C). Hydration numbers for the sample NI-A at low (20 °C) and high (40 °C) temperatures are about 7.5 (1.2 g/g) and 3 (0.48 g/g), respectively. The numerical values in the parentheses denote weight of hydrated water bound to 1 g of NiPAM. Gradual decrease in the hydration number at higher temperatures (~40 °C) might be due to the decrease of the hydrophilic hydration surrounding the amide bond region, since the NiPAM chain has a hydrophobic part of an isopropyl group and a hydrophilic part of an amide bonding. Amide bondings adjacent to isopropyl groups may work as a hydrophilic shell to protect the hydrophobic assembly formed by isopropyl groups, similar to the micellar formation of amphiphilic molecules. Therefore, the hydration number at high temperatures should be related mainly to the hydrophilic hydrated water. It has been known that amino and carboxyl groups contribute to the hydration behavior in an inverse manner respectively, and the hydration of glycine, a molecule with both groups, is sufficiently weak [58]. The present hydration number of ca. 3 at high temperature is a reasonable result. Therefore, the difference in hydration numbers between low and high temperature regions could be assigned dominantly as the number of water molecules liberated by forming the hydrophobic self-assemblies. By extrapolating to the transition region (~32 °C) both from the low and high temperature regions, the magnitude was estimated as ca. 2.5. That is, as a whole, 2.5 water molecules per one NiPAM monomer unit are liberated as free and unbound water molecules during the hydrophobic self-assembly formation. This is, of course, the averaged value; all the NiPAM monomer units do not always take part in such hydrophobic self-assembly, and there may still remain a few NiPAM units dispersed without assembly even at high temperatures. Lele et al.

[29] predicted the bound water content in the NiPAM gel based on the extended lattice-fluid hydrogen-bond theory. They concluded that the bound water content above the volume phase transition point is about 0.4 g/g (hydration number $\sim$ 2.5), whereas it is about 1.6 g/g (hydration number $\sim$10) at low temperature. In the present results, hydration numbers at high (40 °C) and low (20 °C) temperatures are about 3 (0.48 g/g) and 7.5 (1.2 g/g), respectively; fairly good agreement is obtained.

Although the overall characteristics in the temperature dependence are the same for all the three samples, especially for the transition region, a slight difference in magnitudes (lower value for NI-C) is recognized in the low temperature region. This is explainable as follows: the sample of NI-C has a higher BIS content, the average elementary chain length connecting junction points is shorter, and the regions where the junction points gather densely are numerous and/or large (inhomogeneity), and such regions should be less hydrated. On the contrary, at high temperature (>35 °C), all the curves of the hydration number begin to coincide with each other. This coincidence should be responsible for the preparation method of the present gel particles: that is, all gel particles were prepared in the shrunken state at high temperature (60 °C), and the condition of hydration (or, dehydration) should be the same at that condition. If NiPAM gel particles polymerized at a lower temperature than the volume phase transition temperature are available, the direct comparison with the bulk NiPAM gels (polymerized usually at low temperature) is possible and it is very valuable to examine the hydration and dehydration behavior. Such gel particles with sufficiently sharp size distribution are indeed desirable, but unfortunately have not yet been prepared up to the present stage. In addition to this, it is interesting to examine the hydration behavior of NiPAM gel copolymerized with acrylic acid relating to the effect of pH and addition of salt. Such an analysis might give useful information to the weakly charged NiPAM gel.

In addition, the theta temperature of (linear) PNiPAM in water has been reported to be 30.6 °C (a little below the volume phase transition temperature of NiPAM gel) [59]. Change in the decreasing behavior of hydration number (change in the slope) begins even at about 29 °C, the temperature below the volume phase transition temperature. This fact suggests that the hydrophobic regions (isopropyl group) of NiPAM chains begin clustering locally even in that temperature region. This might be the reason why very large two-body interactions take place in aqueous linear PNiPAM solutions, and a very sharp coil-to-globule transition is observed.

Conclusion

Hydration behavior of NiPAM gel particles of submicron size was investigated by means of ultrasonic velocity and density measurements focusing on the hydration properties in response to temperature. Continuous temperature dependence of swelling curves and hydration behaviors were obtained with good reproducibility. Hydration number was quantitatively evaluated in the course of volume phase transition, on the assumption that the NiPAM chain should be desolvated in ethanol-water mixture with proper ethanol composition. Hydration number decreases markedly in the temperature region of the volume phase transition, and the decrease results from the formation of hydrophobic self-assembly and dehydration. Hydration numbers (for the sample NI-A) are about 7.5 (1.2 g/g) and 3 (0.48 g/g) at low (20 °C) and high (40 °C) temperatures, respectively. Self-assembly formation results in the decrease of the hydration number by about 2.5. Hydration number is independent of the size and composition of gel particles in the shrunken state, but a slight dependency was observed in the swollen state. It was also found that the hydrophobically dehydrated assemblies formed in the NiPAM gel particles are more bulky than that in the hydrophobically hydrated state at the low temperature, where the individual NiPAM monomer units disperse separately.

Acknowledgements We are indebted to Prof. K. Nakamura of Rakuno Gakuen University for his helpful advice on the measurements of ultrasonic velocity. K.K. thanks the support of the Ministry of Education, Science, Sports, Culture, and Technology, Japan.

References

1. Tanaka T (1978) Phys Rev Lett 40:820
2. Tanaka T (1981) Sci Am 244:124
3. Annaka M, Tanaka T (1992) Nature (London) 355:430
4. Schild HG (1992) Prog Poly Sci 17:163
5. Shibayama M, Tanaka T (1993) Adv Polym Sci 109:1
6. DeRossi D, Kajiwara K, Osada Y, Yamauchi A (ed) (1989) Polymer gels—fundamentals and biomedical applications. Plenum Press, New York
7. Hoffman AS (2002) Adv Drug Deliv Rev 43:3
8. Stockmayer WH (1960) Makromol Chem 35:54
9. Ptitsyn OB, Kron AK, Eizner YY (1968) J Polym Sci C 16:3509
10. Lifshitz L M, Grosberg AY, Khokhlov AR (1978) Rev Mod Phys 50:683
11. Fujishige S, Kubota K, Ando I (1989) J Phys Chem 93:3311
12. Schild HG, Tirrell DA (1990) J Phys Chem 94:4352

13. Kubota K, Fujishige S, Ando I (1990) J Phys Chem 94:5154
14. Wu C, Wang X (1998) Phys Rev Lett 80:4092
15. Wu C (1998) Polymer 38:4609
16. Tiktopulo EI, Bychkova VE, Rieka J, Ptistyn OB (1994) Macromolecules 27:2879
17. Tokuhiro T, Amiya T, Mamada A, Tanaka T (1991) Macromolecules 24:2936
18. Winnik FM (1990) Macromolecules 23:233
19. Wang X, Qiu X, Wu C (1998) Macromolecules 31:2972
20. Lee L-T, Cabane B (1997) Macromolecules 30:6559
21. Winnik FM, Ottaviani MF, Bossman SH, Pan W, Garcia-Garibay M, Turro NJ (1993) Macromolecules 26:4577
22. Maeda Y, Higuchi T, Ikeda I (2000) Langmuir 16:7503
23. Birshtein TM, Pryamitsyn VA (1991) Macromolecules 24:1554
24. Grosberg AY, Kuznetsov DV (1992) Macromolecules 25:1970
25. Nakata M, Nakagawa T (1997) Phys Rev E 56:3338
26. Nakata M, Nakagawa T (1999) J Chem Phys 110:2703
27. Asano M, Winnik FM, Yamashita T, Horie K (1995) Macromolecules 28:5861
28. Suetoh Y, Shibayama M (2000) Polymer 41:505
29. Lele AK, Hirve MM, Badiger MV, Mashelkar RA (1997) Macromolecules 30:157
30. Herrera-Gomez A, Velazquez-Cruz G, Martin-Polo MO (2001) J Appl Phys 89:5431
31. Pusey PN, van Megen W (1989) Phys A 157:705
32. Shibayama M, Shirotani Y (2000) J Chem Phys 112:442
33. Murray MJ, Snowden M (1995) Adv Colloid Interface Sci 54:73
34. Pelton R (2000) Adv Colloid Interface Sci 85:1
35. Saunders BR, Vincent B (1999) Adv Colloid Interface Sci 80:1
36. Tanaka T, Fillmore DJ (1979) J Chem Phys 70:1214
37. Ito S (1989) Kobunshi Ronbunsyu 46:437
38. Shiio H, Yoshihashi H (1954) J Am Chem Soc 77:4980; Shiio H, Ogawa T, Yoshihashi H (1958) J Am Chem Soc 80:70
39. Hoiland H, Holvik H (1978) J Solution Chem 7:587
40. Koda S, Yamashita K, Iwai S, Nomura H, Iwata M (1994) Polymer 35:5626
41. Hirotsu S,Yamamaoto I, Matsuo A, Okajima T, Furukawa H, Yamamoto T (1995) J Phys Soc Jpn 64:2898
42. Kalyansundaram S, Sundaresan B, Hemalatha J (2001) J Polymer Mater 19:211
43. Zhu PE, Napper DH (1996) J Colloid Interface Sci 177:343
44. Saunders BR, Crowther HM, Morris GE, Mears SJ, Cosgrove T, Vincent B (1999) Colloid Surfaces A 149:57
45. Chu B (1991) Laser light scattering, 2nd edn. Academic, New York
46. Brown W (1993) Dynamic light scattering. Clarendon Press, Oxford
47. Mitaku S, Sakanishi A, Ikegami A (1975) Jpn J Appl Phys 14:395
48. Kogure H, Kubota K (2001) Trans Mater Res Soc Jpn 26:691
49. Greenspan M., Tschiegg CE (1957) J Res Nat Bureau Stand 59:249
50. Snowden M, Chowdhry BZ, Vincent B, Morris G.E (1996) J Chem Soc Faraday Trans 92:5013
51. Horie K, Yamada S, Machida S, Takahashi S, Isono Y, Kawaguchi H (20039 Macromol Chem Phys 204:131
52. Gao J, Frisken B (2003) Langmuir 19:5212
53. Tam KC, Ragaram S, Pelton RH (1994) Langmuir 10:418
54. Kaneshina S, Tanaka M, Tomida T, Matsumura R (1974) J Colloid Interface Sci 48:45
55. Nishikido N, Shinozaki M, Sigihara G, Tanaka M (1981) J Colloid Interface Sci 82:352
56. Kunugi S, Takano K, Tanaka N, Suwa K, Akashi M (1997) Macromolecules 30:4499
57. Kunugi S, Yamazaki Y, Takano K, Tanaka N, Akashi M (1999) Langmuir 15:4056
58. Ishimura M, Uedaira H (1990) Bull Chem Soc Jpn 63:1
59. Kubota K, Fujishige S, Ando I (1990) Polym J 22:15